Astron. Astrophys. 316, 323–332 (1996)

ASTRONOMY
AND
ASTROPHYSICS

The quasi-parallel shock wave detected by Ulysses on day 92:109

J. A. González-Esparza[1], **E. J. Smith**[1], **A. Balogh**[2], **and J. L. Phillips**[3]

[1]Jet Propulsion Laboratory, California Institute of Technology, Mail Stop 169-506, 4800 Oak Grove Drive, Pasadena, CA 91109-8099, USA
[2]Imperial College, The Blackett Laboratory, Prince Consort Road, London SW7 2BZ, UK
[3]Los Alamos National Laboratory, Los Alamos, New Mexico, USA

Received 19 February 1996 / Accepted 15 May 1996

Abstract. On day 92:109, at about 5.4 AU and 9° south, Ulysses detected a strong quasi-parallel shock wave leading an interaction region. We describe this singular event on different temporal scales, placing emphasis on the magnetic field observations. The solar wind preceding the shock presented very unusual long-lived conditions: for about one day the interplanetary magnetic field was closely radially oriented and this was associated with a strong anisotropy in proton temperature ($T_{p_\parallel}/T_{p_\perp} < 1$). The wave activity in the upstream and downstream regions have the largest spatial extent for any interplanetary shock wave reported before. In the foreshock region we identified 10^{-2} Hz waves and continual distributions of backstream ions up to 28.5 hours ($\geq$ 0.29 AU) ahead of the shock. The downstream region was characterized by large amplitude, low frequency ($f \leq 10^{-3}$ Hz), compressive perturbations for about 34 hours. The temporal fluctuations around the shock transition do not allow us to apply the techniques based on the Rankine-Hugoniot relations to infer the shock parameters.

Key words: solar system: interplanetary medium – shock waves – waves

1. Introduction

On the basis of diverse studies from the quasi-parallel region of the Earth's foreshock, there is a well-known ULF wave associated with beams of backstreaming suprathermal ions (∼KeV) (see, e.g., Russell and Hoppe 1983). These large amplitude left-handed waves with frequencies close to 0.03 Hz in the spacecraft frame are correlated with different types of backstreaming ions (Hoppe et al. 1981): intermediate (Paschmann et al. 1981), diffuse (Gosling et al. 1978a), and gyrating (Thomsen et al. 1985). Gosling et al. (1984) reported that backstream ions are also observed at the front of transient, forward, interplanetary shocks at 1 AU, but their velocity distributions are relatively structureless, and the particle fluxes are less intense. The aim of this paper is to describe a quasi-parallel, interplanetary, shock wave detected by Ulysses with the longest spatial extent of upstream and downstream wave activity reported in the literature. The upstream waves with frequencies about 10^{-2} Hz were associated with continual distributions of gyrating ion beams detected in the foreshock region (Huddleston et al., unpublished manuscript, 1995). The characteristics of this event presented conditions that are not available in the foreshock region of the Earth's bow shock.

Interplanetary shocks, in general, are weaker (their Mach numbers are less than 3) and larger (they have spatial extents and radii of curvature of the order of astronomic units) than the Earth's bow shock. As their shock front is less curved, one of the reasons to study interplanetary shocks is that their simpler geometry allow us, in principle, to understand better the diverse physical phenomena associated with the θ_{B_n} of low Mach number shocks. Within 1 AU most of the interplanetary shocks are transient forward shocks associated with ejecta, while beyond 2 AU most of the interplanetary shocks are caused by interaction regions.

The most studied quasi-parallel, interplanetary, shock wave in the literature is the transient forward shock detected on 11-12 November 1978 by ISEE 1, 2 and 3 at 1 AU. Kennel et al. (1984a,b) presented a comprehensive overview of the magnetic, solar wind plasma, and plasma wave observations of this event. The shock detected by ISEE and the shock reported here were caused by different heliospheric phenomena and observed at different heliocentric distances. As we will show it, our event had very different characteristics.

2. Event 92:109

The event was observed on day 92:109, two months after the Jupiter flyby, at about 5.4 AU and 9° south. We will discuss, from different temporal scales, the observations by the magnetic field and solar wind plasma experiments described by Balogh et al. (1992) and Bame et al. (1992) respectively. The magnetic field data has a temporal resolution of 1 or 2 seconds, while the solar wind plasma data ($\mathbf{V}_{sw}, N_p, T_p$) has a temporal resolution of about 4 or 8 minutes. We begin from the large-scale features,

Send offprint requests to: J. A. González-Esparza

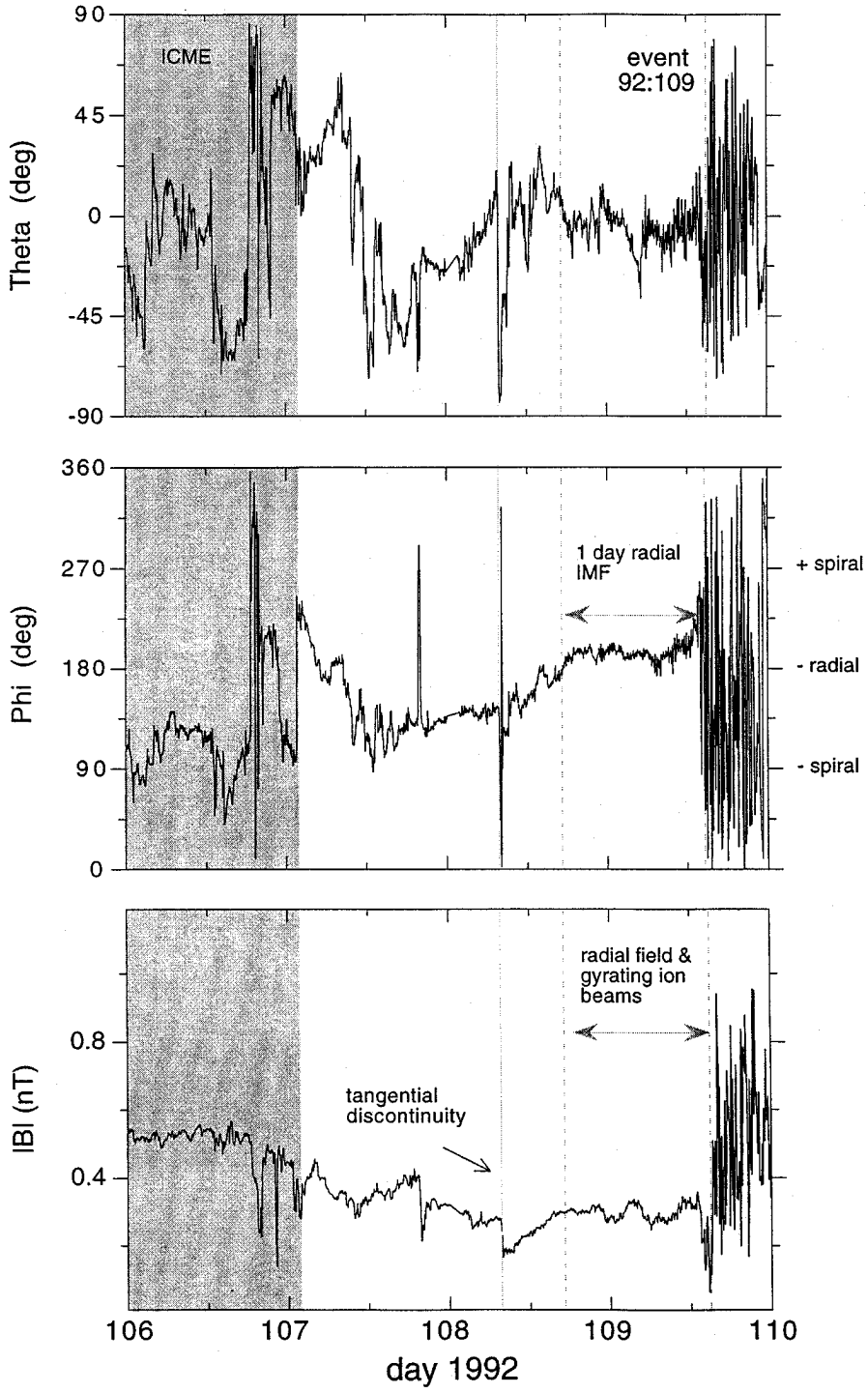

Fig. 1. Four-day plot of interplanetary magnetic field (IMF) magnitude and direction from day 92:106 to day 92:110. After the passing of the interplanetary counterpart of coronal mass ejection (ICME) the IMF had an out-of-spiral direction for a few days. For about one day prior event 92:109, the IMF was closely oriented along the radial direction ($\Phi \sim 180^\circ$)

and then we describe some characteristics of the wave activity and the shock transition.

2.1. Large-scale features

After the Jupiter flyby Ulysses detected high rates of transient activity. In fact, a few days before the event 92:109 we detected a large series (6 in number) of interplanetary counterparts of coronal mass ejections (ICMEs) (González-Esparza et al. 1996). Figure 1 shows four-day plots of the two polar angles and magnitude of the interplanetary magnetic field (IMF) preceding event 92:109. At the left side of Fig. 1, identified by a bidirectional streaming of suprathermal electrons and other ejecta signatures (J. L. Phillips et al., unpublished manuscript, 1995), is shown the last ICME detected before the event 92:109. The mid-panel shows the plot of the IMF longitudinal angle Φ. At 5 AU the Parker's spiral close to the ecliptic plane is tighten and Φ is about 90° or 270°. However, after the ICME, Φ loosed

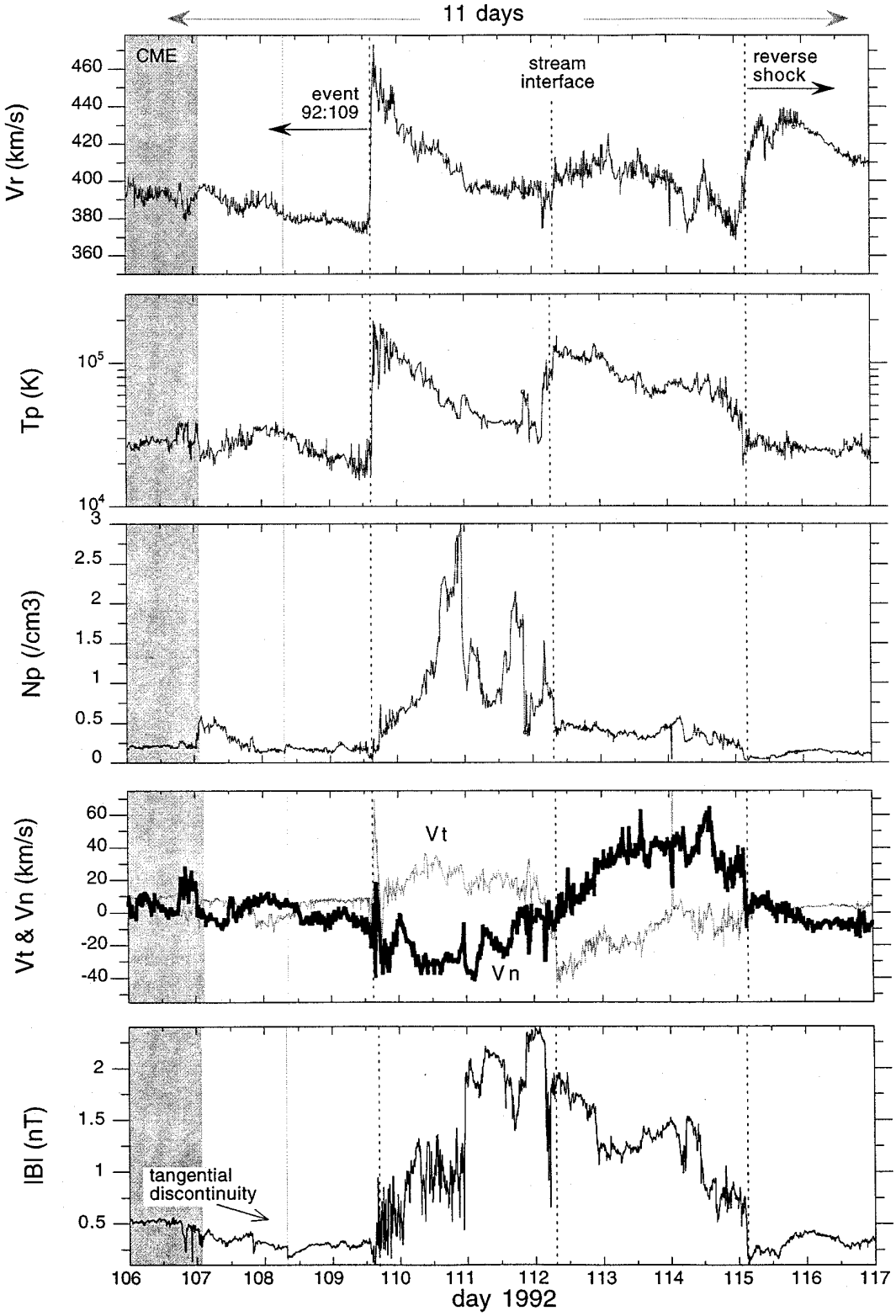

Fig. 2. Eleven-day plot of IMF and solar wind plasma parameters. This well-defined interaction region (led by event 92:109) was detected about two months after the Jupiter fly-by. The strong south-north shear flow in V_n at the stream interface suggest that the front of the interaction region was pointing southerd and the trailing edge (92:115) was pointing northerd (Pizzo 1991)

its spiral orientation for a few days. On day 92:108 there was a strong tangential discontinuity at about 9:00 hours, and from about 15:00 hours the IMF became radially oriented ($\Phi \sim 180°$) lasting for about one day. This long-lived out-of-spiral orientation of the IMF is very unusual. What caused this behavior of the IMF?

Figure 2 shows eleven-day plots of the interaction region led by event 92:109. The solar wind bulk speed $V_{\rm r}$, the proton temperature Tp, the proton density Np, and the IMF magnitude $|B|$ all show a well-defined interaction region. Inside the interaction region the stream interface is dividing both compressed slow and fast solar winds. The two non-radial components of the solar wind velocity ($V_{\rm t}, V_{\rm n}$) show the characteristic strong shear flow at the stream interface (Gosling et al. 1978b). The compressed fast solar wind had a positive $V_{\rm n}$ (northern); while the compressed slow solar wind had a negative $V_{\rm n}$ (southern). This north-south flow deflection at the stream interface implies that the interaction region was tilted with respect to the solar equator (Pizzo 1991). The front of the interaction region (92:109) was pointing southward and its trailing edge (92:115) was pointing northward.

Besides the unusual IMF in Fig. 1, the large-scale observations of the interaction region presented two peculiarities: (1) Gosling et al. (1993b) reported that most of the corotating shocks detected by Ulysses beyond 2 AU were characterized by enhanced fluxes of suprathermal electrons in the foreshock region. However, the leading edge of this interaction region did not include any electron foreshock. (2) The velocity plot at the top of Fig. 2 shows that the shocked slow solar wind on day 92:109 was faster than the ambient fast solar wind (right side of Fig. 2); whereas the shocked fast solar wind on day 92:115 had a similar speed than the ambient slow solar wind (left side of Fig. 2). This suggests that the front and trailing edges of this interaction region were propagating over the rarefaction zones that precede and follow the interaction regions (see, e.g., Hu (1993)).

2.2. Upstream waves

The characteristics of the solar wind plasma associated with the radially oriented IMF (Fig. 1) were very stable. The alfvénic $V_{\rm A}$ (= $|B|/(\mu_{\rm o} N_{\rm p} m_{\rm p})^{1/2}$) and the sonic $c_{\rm s}$ (= $(kT/N_{\rm p}m_{\rm p})^{1/2}$) speeds were both about 15 kms^{-1}; the proton gyrofrequency $\Omega_{\rm p}$ (= $(e|B|/\epsilon_{\rm o} N_{\rm p} m_{\rm p})^{1/2}$) was about 0.02–0.03 Hz; and the plasma β (= $\frac{NkT}{B^2/2\mu_{\rm o}}$) was about 1. Associated with this region it was reported that from about 10:30 hours on day 92:108 (after the tangential discontinuity in Figs. 1 and 2) to about 13:00 hours on day 92:109 there was a strong but indeterminate anisotropy in proton temperature ($T_{p_\parallel}/T_{p_\perp} < 1$) (Huddleston et al., unpublished manuscript, 1995).

Figure 3 shows the one-day plot of event 92:109 in terms of the three IMF components and magnitude in 1-minute averages. The magnetic perturbations shown in the figure have very low frequencies (with periods $\sim$ 15 minutes). The upstream wave activity was detected up to 0.29 AU ($>$ 28 hours) ahead the shock and the downstream waves had a similar extent. These spatial extents are far larger than any other interplanetary shock reported in the literature. We obtained the power spectra of these very low frequency waves ($f \sim 10^{-3}$ Hz) taken from the different intervals denoted by solid lines in Fig. 3. The far upstream intervals ((00:10-13:49 UT) (05:22-09:40 UT)) were dominated by transverse waves ($\delta B_{\rm n}, \delta B_{\rm t}$). Closer to the shock (09:22-13:49 UT) the waves increased their amplitude and $B_{\rm r}$ was also affected by the perturbations. In the downstream region, the perturbations were highly compressive ($\delta|B|$) and increased their amplitude by more that two orders of magnitude with respect to the upstream region. Contrary what we would expect, the far downstream interval (19:27-23:48 UT) showed larger perturbations than the closer downstream interval (15:23-19:07 UT) suggesting that another physical phenomena might be taking place. At the stream interface (shown in Fig. 2 but not shown in Fig. 3) the downstream wave activity ceased and the IMF recovered its normal spiral orientation. How were these very extended low frequency perturbations produced?

In a way similar to that reported for the foreshock region of the Earth's bow shock (Fairfield 1969; Hoppe et al. 1981, 1982; Thomsen et al. 1985; Blanco-Cano and Schwartz, 1995), and for interplanetary shocks (Tsurutani et al. 1983; Kennel et al. 1984a; Russell et al. 1985), we found continual intervals with ULF waves (10^{-2} Hz) associated with the backstream ion beams reported by Huddleston et al. (unpublished manuscript, 1995). Figure 4 shows magnetic field data in high-time resolution with an example of the 10^{-2} Hz waves that we detected in the foreshock region. In this case (top of Fig. 4) the perturba-

Table 1. Wave characteristics at different intervals in the foreshock region: (1) time interval; (2) main frequency in the spacecraft frame; (3) angle between the propagation direction and the averaged magnetic field[a]; (4) polarization in the spacecraft frame; (5) average field magnitude; (6) compressional amplitude (amplitude of the fluctuations in the field's magnitude), and (7) normalized compressional amplitude

Time, UT (h:min)	Frequency (Hz)	$\theta^{\rm a}_{\hat{k}B}$	Polarization	$\lvert B\rvert$ (nT)	δB (nT)	$\delta B/B$
Day 92:108						
10:48–10:56	0.03	$20° \pm 7°$	RH	0.142	0.004	0.03
15:21–15:33	0.06	$90° \pm 1°$	RH	0.191	0.04	0.2
16:24–16:29	0.07	$90° \pm 1°$	RH	0.193	0.04	0.2
21:59–22:04	0.05	$89° \pm 1°$	LH	0.218	0.05	0.2
22:53–22:59	0.05	$87° \pm 10°$	RH	0.216	0.05	0.2
23:41–23:47	0.04	$74° \pm 14°$	LH	0.183	0.04	0.2
Day 92:109						
04:23–04:31	0.03	$30° \pm 10°$	LH	0.229	0.015	0.06
06:14–06:34	0.04	$24° \pm 9°$	RH	0.172	0.04	0.2
07:20–07:21	0.05	$72° \pm 15°$	RH	0.170	0.04	0.2
09:41–09:47	0.04	$20° \pm 1°$	RH	0.204	0.04	0.2
14:47–14:57	0.05	$84° \pm 5°$	LH	0.222	0.05	0.2

[a] BANAL estimates the wave progation direction by two different methods: (1) Means' (*J. Geophys. Res., 77,* 5551, 1972), and (2) minimum variance analysis. We report the averaged value based on the results by the two methods.

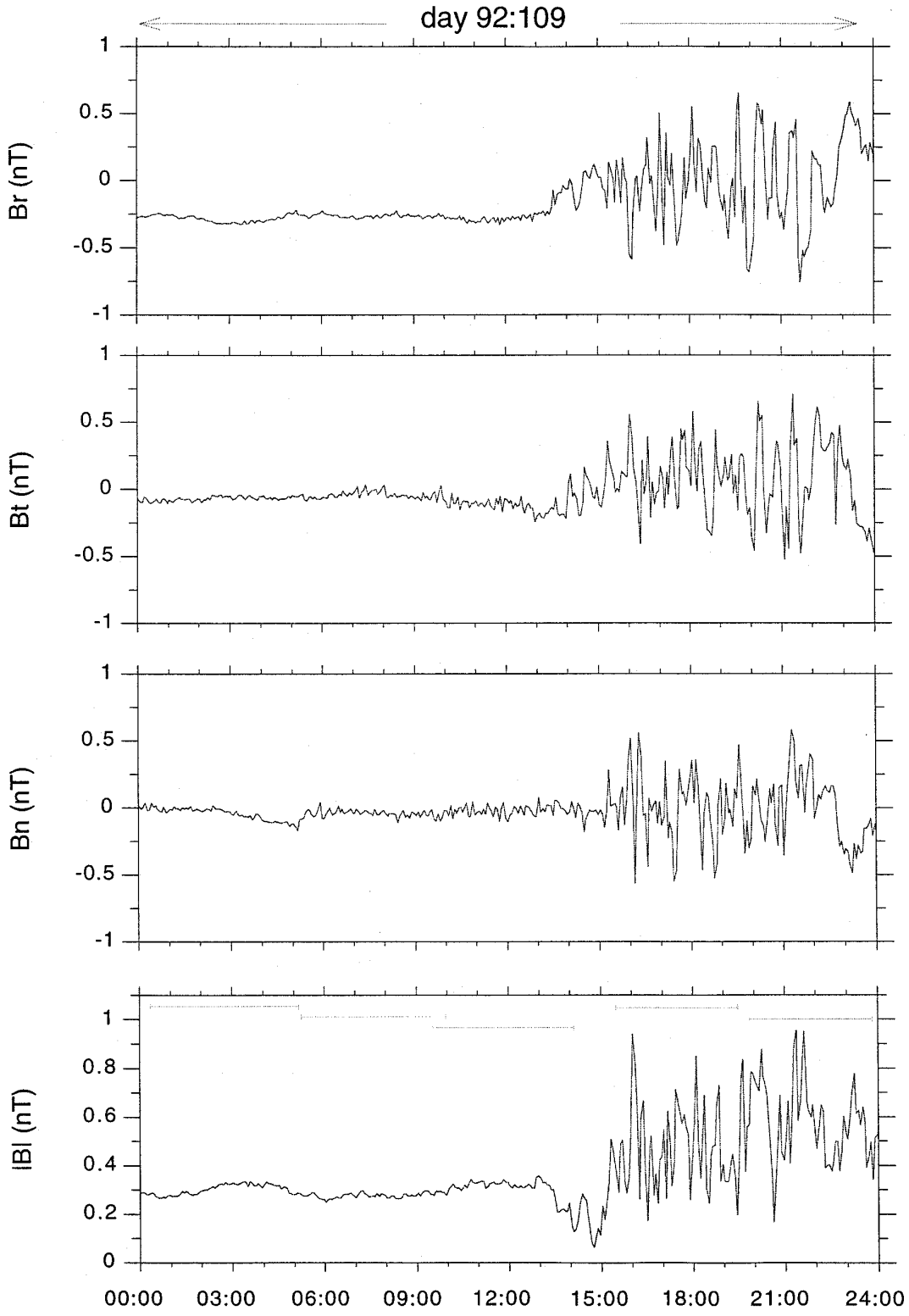

Fig. 3. One-day plot of the three IMF components and magnitude on day 92:109. The data is in one-minute averages. The radial IMF connected the shock to very extended distances in the upstream region producing the largest pattern of wave activity for an interplanetary shock ever reported

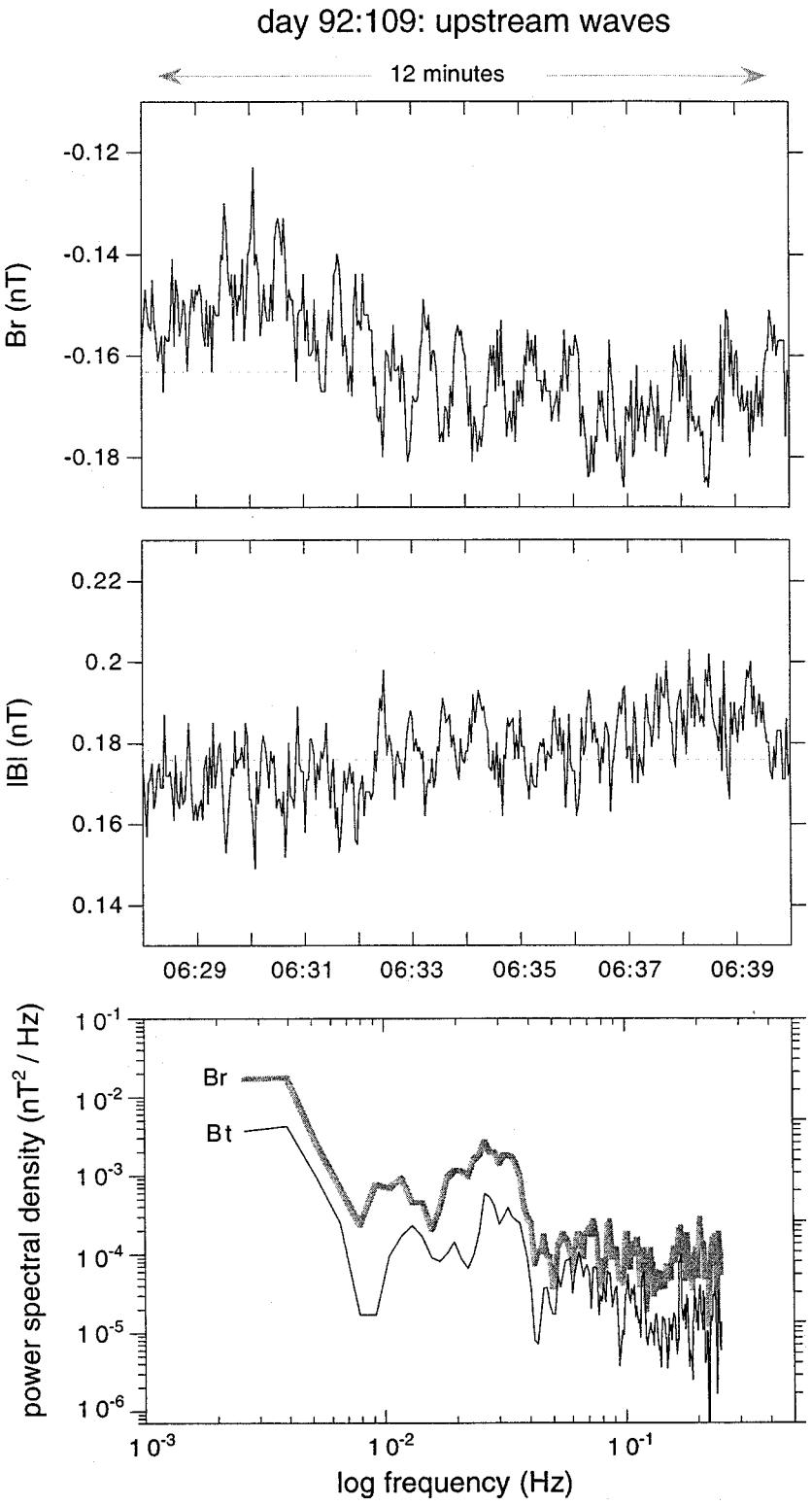

Fig. 4. An example of low frequency (10^{-2} Hz) waves detected in the foreshock region on day 92:109 (see Table 1). The IMF data is in high-temporal resolution (1 vector per second). The lower panel shows the power spectra analysis of this interval

tion was clearly noticeable in B_r and $|B|$. The lower panel of Fig. 4 shows the power spectrum analysis of this interval with a clear peak around 2-4 $\times 10^{-2}$ Hz. Table 1 shows some intervals with 10^{-2} Hz waves that we found by visual inspection of our high time resolution data. We used the University of California, Los Angeles (UCLA) routine BANAL to determine some of the properties of these perturbations. The first interval with wave activity was recognized as far as about 28.5 hours before the shock encounter (the first beam of backstream ions was found at about 14:00 hours on day 92:108). Most of these waves were right-hand polarized in the spacecraft frame and their weighted frequencies varied between 0.03-0.07 Hz.

Further study of these waves and the backstream ion distributions will provide information of the evolution of the backstream ion beams and how is associated with the wave activity in a scale and geometry that cannot be studied at 1 AU.

2.3. Shock local parameters

From the large-scale point of view (Fig. 2) event 92:109 satisfies all the familiar signatures attributed to a fast MHD shock, i.e., compressive jumps in V_r, T_p, N_p and $|B|$. The radially oriented IMF, the strong wave activity, and the backstreaming ions detected before the shock suggest that this was a quasi-parallel shock. We checked the Ulysses' common data pool and corroborated that there were impulsive electric field bursts in VLF plasma waves (2–8, 0.5–2 kHz V^2 m^2) and energetic particle enhancements typically found in the upstream region of quasi-parallel interplanetary shocks (Kennel el at. 1982). However, at high temporal resolution the event looks different. Figure 5 shows four-hour plots of plasma and IMF parameters in high time resolution (the magnetic field data has about 240 times higher temporal resolution than the plasma data). Identified by the jumps in V_r and T_p at the top of the figure, the shock occurred somewhere between 15:06-15:10 hours. However, the jumps in N_p and $|B|$ are ill-defined with strong discontinuities around the shock transition. From 13:00 to 15:00 hours (upstream region), N_p presented fluctuations which seem to be in phase with fluctuations in $|B|$ (this is not the case in the downstream region). In Fig. 1 we pointed out a very stable radially oriented IMF for several hours preceding event 92:109, but in Fig. 5 the IMF direction has many discontinuities and between 14:00 to 15:00 hours Φ had contrasting orientations for periods of several minutes. At the bottom of Fig. 5 the proton β_p and the entropy per proton S_p (= $k \ln[T_p^{1.5}/N_p]$) show paradoxical behaviors. Between 14:30 and 15:00 hours, associated with the low value of $|B|$, β_p was very high (up to 12) and just after the shock β_p was about 1. On the other hand, S_p did not show a well-defined increment after the shock jump.

The problem of inferring the shock local parameters from in-situ single spacecraft measurements is well known (see, e.g., Viñas and Scudder 1986). Table 2 shows some averaged upstream and downstream solar wind parameters for the two shaded regions in Fig. 5 defined by the three closest plasma points before and after the shock jump. The values of $\bar{V}_r$, $\bar{T}_p$, $\bar{N}_p$, and $|\bar{B}|$, all show clear increments after the shock, nevertheless the temporal variations and the arbitrary intervals selected. However, $\bar{\beta}_p$ decreases and $\bar{S}_p$ does not to change. In the Rankine-Hugoniot solutions β_p and S_p are always increased after the shock (see, e.g., Kennel et al. 1985 Fig. 5; and Whang et al. 1990). In this case the solar wind measurements before and after the shock jump are not related by the stationary Rankine-Hugoniot equations. The temporal fluctuations in both upstream and downstream regions and the low temporal resolution of our plasma data, do not allow us to apply the known techniques based on the Rankine-Hugoniot relations to infer the shock parameters. In order to study the physical phenomena associated with this event we need to infer the approximated values of the shock parameters by other methods, in a similar way as we study the quasi-parallel region of the Earth's bow shock. For example, we could use the global geometry of the interaction region, deduced from the stream interface, to infer the shock normal direction. Then the long-lived conditions of the upstream region with allow us to approximated θ_{B_n} and M.

Table 2. Upstream and downstream averaged solar wind parameters

Parameter	Units	Value upstream[a]	Value downstream[b]
Solar wind bulk velocity V_r	[km s^{-1}]	406 ± 12	445 ± 4
Proton temperature T_p	[10^4 K]	2.32 ± 0.07	5.91 ± 1.2
Proton density N_p	[cm^{-3}]	0.06 ± 0.05	0.18 ± 0.08
IMF magnitude B[c]	[nT]	0.22 ± 0.1	0.41 ± 0.18
Proton beta β_p		2.7 ± 2	1.2 ± 0.4
Entropy per proton S_p	[10^{22}J K^{-1}]	1.05 ± 0.06	1.05 ± 0.03
Alfvén speed V_A	[km s^{-1}]	15 ± 8	29 ± 5
Sonic speed c_s	[km s^{-1}]	14 ± 0.2	22 ± 2
Larmor radius r_L	[10^3 km]	24 ± 7	37 ± 8
Proton gyrofrequency Ω_p^c	[10^{-2}rad s^{-1}]	2.1 ± 0.1	3.9 ± 1.7

[a] On the basis of the three plasma measurements from 14:58 to 15:06 hours

[b] On the basis of the three plasma measurements from 15:10 to 15:18 hours

[c] Averaged from high-time resolution IMF data over the same time interval

2.4. Shock transition

Figure 6 shows thirty-minute plots of high time resolution IMF data around the shock transition. The shock plane is not well defined. The temporal fluctuations do not allow us to apply magnetic coplanarity to infer the shock's normal direction and θ_{B_n}. The shaded regions in Fig. 6 correspond to the same regions in Fig. 5 and Table 2. Between these two regions there is an interval of approximately four minutes with low IMF magnitude and with magnetic structures that might be magnetic pulsations or short, large amplitude, magnetic structures (SLAMS) that have been reported at the quasi-parallel shock transition of the Earth's bow shock (Thompsen et al. 1990; Schwartz and Burgess 1991; Schwartz et al. 1992). These structures are associated with the unstable nature of supercritical quasi-parallel shocks (Burgess 1989). We studied the magnetic hodograms of these structures

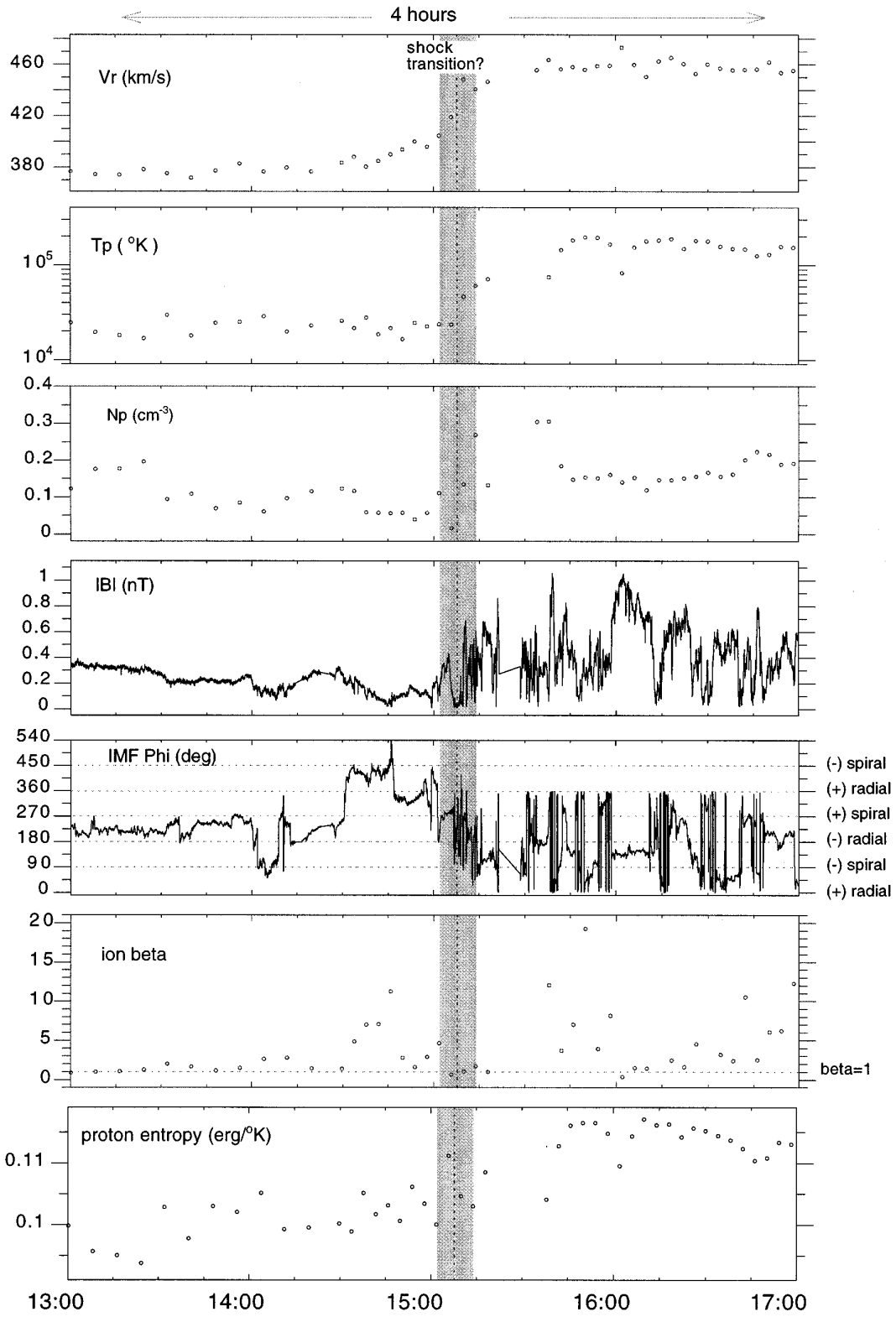

Fig. 5. Four-hour plot of solar wind plasma and IMF parameters of event 92:109. Contrary to the strong shock that we might expect from Fig. 2, the plasma parameters present just a small jump. The proton entropy S_p and proton β_p both show paradoxical behaviors associated with a shock wave

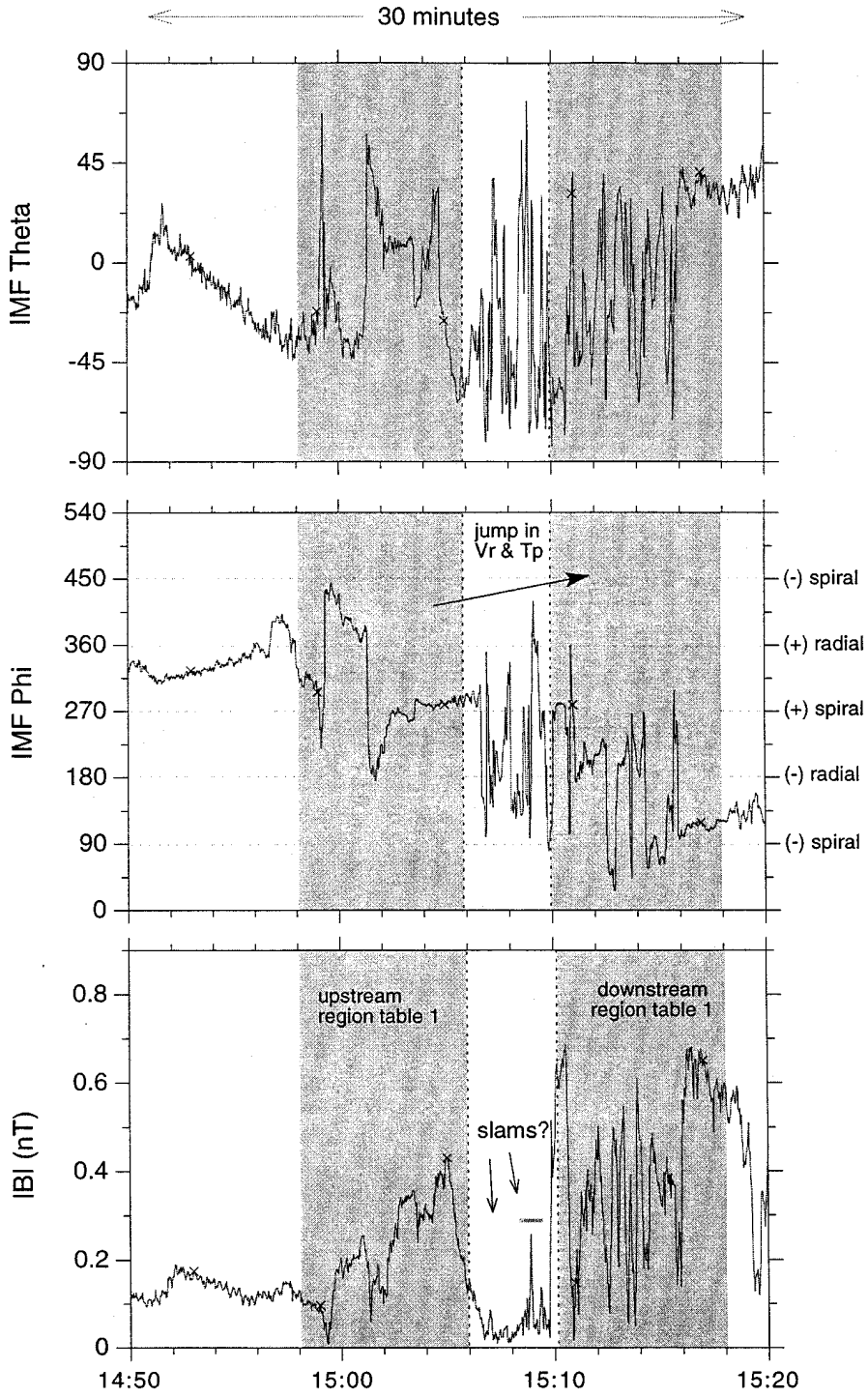

Fig. 6. Thirty-minute plots of IMF data in high-temporal resolution (1 vector per second) around the shock transition. We cannot apply magnetic coplanarity to infer the shock normal and θ_{B_n}. The shadow upstream and downstream intervals are the same regions of Fig. 5

and we corroborated that they present similar polarization trends to that of other SLAMS (Schwartz et al. 1992). It is possible that when Ulysses was crossing the shock, the shock was in the process of reforming. This might explain the local variations, the magnetic structures, and why we did not find a well-defined shock transition. However, these phenomena that are commonly observed in the quasi-parallel crossing of the Earth's bow shock are not expected in a corotating shock in the outer heliosphere.

3. Summary

We have reported a exceptional interplanetary shock wave. There is not any other shock with similar spatial extents in wave activity in the whole set of Ulysses observations and we are not aware of a similar event in the Pioneer 10 and 11 and Voyager 1 and 2 observations. The large-scale context of this quasi-parallel shock provide an opportunity for further study in a scale and geometry that are rarely available.

Acknowledgements. We are grateful to Richard Nelson and Xochitl Blanco-Cano for reading the manuscript. The critical reading by the referee is appreciated. J. A. G-E. is grateful to the National Research Council for financial support at JPL as a Resident Research Associate. The research at Jet Propulsion Laboratory, California Institute of Technology, was supported by the National Aeronautics and Space Administration.

References

Balogh, A., Beek T.J., Forsyth R.J., et al., 1992, A&AS 92, 221
Bame S.J., McComas D.J., Barraclough B.L., et al., 1992, A&AS 92, 237
Blanco-Cano X., Schwartz S.J., 1995, Adv. Space Res. 15, 97
Burgess D., 1989, Geophys. Res. Lett. 39, 345
Burton M.E., Smith E.J., Balogh A., et al., this issue
Fairfield D.H., 1969, J. Geophys. Res. 74, 3541
Fuselier S.A., Thomsen M.F., Gosling J.T., et al., 1986, J. Geophys. Res. 91, 91
González-Esparza J.A., Balogh A., Forsyth R.J., et al., 1996, J. Geophys. Res. 101, 17057
Gosling J.T., Asbridge J.R., Bame S.J., et al., 1978a, J. Geophys. Res. 5, 957
Gosling J.T., Asbridge J.R., Bame S.J., et al., 1978b, J. Geophys. Res. 83, 1401
Gosling J.T., Bame S.J., Feldman W.C., et al., 1984, J. Geophys. Res. 89, 5409
Gosling J.T., Bame S.J., McComas D.J., et al., 1993a, J. Geophys. Res. 20, 2789
Gosling J.T., Bame S.J., Feldman W.C., et al., 1993b, J. Geophys. Res. 21, 2335
Hoppe M. M., Russell C.T., Frank L.A., et al., 1981, J. Geophys. Res. 86, 4471
Hoppe M. M., Russell C.T., Eastman T.E., et al., 1982, J. Geophys. Res. 87, 643
Hu Y.Q., 1993, J. Geophys. Res. 98, 13201
Kennel C.F., Scarf F.L., Coroniti F.V., et al., 1982, J. Geophys. Res. 87, 17
Kennel C.F., Scarf F.L., Coroniti F.V., et al., 1984a, J. Geophys. Res. 89, 5419
Kennel C.F., Edmiston J.P., Scarf F.L., et al., 1984b, J. Geophys. Res. 89, 5436
Kennel C.F., Edmison J.P., Hada T., 1985, in: Stone R.G., Tsurutani B.T. (eds.), Collisionless Shocks in the Heliosphere. Geophys. Mono. 34, p. 1
Pizzo V.J., 1991, J. Geophys. Res. 96, 5405
Pizzo V.J., 1994, J. Geophys. Res. 99, 4173
Russell C.T., Hoppe M.M., 1983, Space Sc. Rev. 34, 155
Russell C.T., Smith E.J., Tsurutani B.T., et al., 1985, in: Solar Wind Five, NASA Conf. Publ., CP-2280, 385
Schwartz S.J., Burgess D., 1991, J. Geophys. Res. 18, 373
Schwartz S.J., Burgess D., Wilkinson W.P., et al., 1992, J. Geophys. Res. 97, 4209
Thomsen M.F., Gosling J.T., Bame S.J., et al., 1985, J. Geophys. Res. 90, 267
Thompsen M.F., Gosling J.T., Bame S.J., et al., 1990, J. Geophys. Res. 95, 957
Tsurutani B.T., Smith E.J., 1982, J. Geophys. Res. 87, 7389
Tsurutani B.T., Smith E.J., Jones D.E., 1983, J. Geophys. Res. 88, 5645
Viñas A.F., Scudder J.C., 1986, J. Geophys. Res. 91, 39
Whang Y.C., Liu S., Burlaga L.F., 1990, J. Geophys. Res. 95, 18769